

# Toxicology Research

Accepted Manuscript



This is an *Accepted Manuscript*, which has been through the Royal Society of Chemistry peer review process and has been accepted for publication.

*Accepted Manuscripts* are published online shortly after acceptance, before technical editing, formatting and proof reading. Using this free service, authors can make their results available to the community, in citable form, before we publish the edited article. We will replace this *Accepted Manuscript* with the edited and formatted *Advance Article* as soon as it is available.

You can find more information about *Accepted Manuscripts* in the [Information for Authors](#).

Please note that technical editing may introduce minor changes to the text and/or graphics, which may alter content. The journal's standard [Terms & Conditions](#) and the [Ethical guidelines](#) still apply. In no event shall the Royal Society of Chemistry be held responsible for any errors or omissions in this *Accepted Manuscript* or any consequences arising from the use of any information it contains.

For Toxicology Research

## **A Gene Signature for Gold Nanoparticle-Exposed Human Cell Lines**

Ruei-Yue Liang<sup>a</sup>, Hsin-Fang Tu<sup>b</sup>, Xiaotong Tan<sup>a</sup>, Yu-Shan Yeh<sup>c</sup>, Pin Ju Chueh<sup>a</sup> and Show-Mei Chuang<sup>\*a</sup>

<sup>a</sup>Institute of Biomedical Sciences, National Chung Hsing University, Taichung, 40227, Taiwan

<sup>b</sup>Bachelor Program of Biotechnology, National Chung Hsing University, Taichung, 40227, Taiwan

<sup>c</sup>Center for Measurement Standards (CMS), Industrial Technology Research Institute (ITRI), Hsinchu, 30011, Taiwan

\* Correspondence: Dr. Show-Mei Chuang, Institute of Biomedical Sciences, National Chung Hsing University, Taichung, 40227, Taiwan. Tel: +886 4 22840896. Fax: +886 4 22853469. E-mail: [smchuang@dragon.nchu.edu.tw](mailto:smchuang@dragon.nchu.edu.tw)

## Abstract

There is currently a significant need for effective methods aimed at diagnosing and screening for nanoparticle exposure. We previously investigated the toxicity of three different particle sized gold nanoparticles (AuNPs) toward different types of mammalian cells and explored a related gene expression profile by cDNA microarray analysis of AuNP-exposed MRC-5 cells. In this study, we sought to further identify genes that could be used as biomarkers for AuNP exposure. We used cDNA microarray analysis to obtain comprehensive gene expression profiles from A549 cells exposed to three different-sized AuNPs. A total of 409 genes were commonly up-regulated by the tested AuNPs; of them, 71 had previously been analyzed to be up-regulated in MRC-5 cells. Among the top-ranked 30 of these 71 up-regulated genes, based on magnitude of induction, nine genes were confirmed to be transcriptionally induced in A549 cells by all three tested AuNPs, as assessed by quantitative real-time polymerase chain reaction (qPCR). Among them, *TSC22D3*, *TRIB3*, *PCK2* and *DDIT4* were the most sensitive to the three AuNPs, and showed dose-dependent changes in several human cell lines. qPCR and immunoblotting analyses revealed that the same concentrations of micro-Au and nano-TiO<sub>2</sub> failed to elicit up-regulation of these four genes at the mRNA and protein levels in any tested cell lines. Although the definition and practical implementation of specific biomarkers for nanoparticle is still in its infancy, our data suggest that it may be possible to define reliable biomarkers for the diagnosis of nano-material exposure.

Keywords: gold nanoparticle, biomarker, TSC22D3, TRIB3, PCK2, DDIT4

## Introduction

In recent years, nanoparticles (NPs) have been used for a broad variety of biological and biochemical applications<sup>1</sup>. Compared to micro-scale materials, NPs have more adverse effects on organisms, presumably due to their larger reactive surface areas. As the application of NPs in many commercial products continues to increase, concerns have grown regarding their toxicity. However, a lack of characteristic symptoms makes it difficult to diagnose the early stages of NP exposure. Therefore, we need to establish more effective methods for diagnosing and screening for NP exposure, in the hopes of improving early detection, treatment strategies and patient outcomes.

Traditionally, chronic exposure of animals to nano-materials has been used to predict human health risks and the potential for tumor induction<sup>2-7</sup>. However, this approach can be so time consuming that its usefulness is limited. Thus, rapid and sensitive new strategies are needed to efficiently detect NP exposure with negligible effect on other materials.

Gene expression profiling is considered to have potential for the rapid and cost-effective assessment of hazards. In recent years, cDNA-microarray-based gene expression profiling has been used for clinical whole-genome screening and biomarker discovery. For example, differentially expressed subsets of genes were identified as being potentially useful for distinguishing groups of colon cancer patients with distinct clinical outcomes<sup>10, 11</sup>. Gene expression profiling has also been used to assess the hazards of exposure to various chemicals<sup>12</sup>, including dibutyl phthalate<sup>13</sup>, acetaminophen<sup>14</sup>, alachlor<sup>15</sup> and dimethylarsenic (DMA)<sup>16</sup>. In nanotechnology, gene expression profiling has been used to examine the effects of exposing mice to various NPs, including those composed of TiO<sub>2</sub><sup>17-19</sup>, ZnO<sup>8</sup> and carbon black<sup>9</sup>. Thus, gene expression profiling can be used to identify key events correlated with adverse outcomes, decipher molecular mechanisms, and predict human diseases.

In recent years, the search for biomarkers of preclinical human disease (particular cancer) has become increasingly important. Reliable biomarkers can be effective for early detection, prognosis, prediction, and treatment-response monitoring, and can allow clinicians to personalize therapies and

improve outcomes. For example, *KRAS* mutations have been associated with carcinogenesis and resistance to anti-epidermal growth factor receptor (EGFR) monoclonal antibody (mAb)-based treatment, and less favorable clinical outcomes and shorter survival have been associated with the presence of *KRAS* mutations at codon 13<sup>20,21</sup>. Other known markers (*e.g.*, *HER2*, *PI3K*, *BRAF*, epigenetic biomarkers, and genetic polymorphisms) are also considered attractive potential biomarkers for the early detection of tumors<sup>11</sup>. In tumor therapy, five levels of evidence (LOE) for determining the clinical validity and utility of a biomarker have been standardized and recommended by the American Society of Clinical Oncology Tumor Markers Guidelines Committee<sup>22,23</sup>. However, suitable clinically relevant diagnostic markers of NP exposure are not currently available, and techniques for accurate diagnosis and proper monitoring have not yet been established. Such work could critically improve the early diagnosis of NP exposure and contribute to risk assessments of engineered nano-materials and manufactured nano-waste. The latter is especially important for individuals working in nanotechnology.

We previously investigated the toxic effects of AuNPs (three particle sizes) in different types of mammalian cells<sup>24</sup> and used cDNA microarray analysis to explore one relevant gene expression profile in AuNP-exposed MRC-5 cells<sup>25</sup>. In the present study, we identify four potential biomarkers for AuNP exposure, show that these gene markers appear to be effective biomarkers of AuNP exposure in several human cell lines (*e.g.*, A549, HEK293, HepG2 and AGS), and reveal that they are not subject to interference from nano-TiO<sub>2</sub> or micro-Au.

## Materials and methods

**Cell Culture.** The human cell lines A549, HEK293 and HepG2 were cultured in DMEM (Invitrogen, Carlsbad, CA, USA) or AGS was cultured in RPMI-1640 (Invitrogen) supplemented with 10% fetal bovine serum (FBS), sodium bicarbonate (2%, w/v), L-glutamine (0.29 mg/ml), penicillin (100 units/ml), and streptomycin (100 µg/ml) (Invitrogen) at 37°C in a humidified 5% CO<sub>2</sub> incubator.

**Antibodies and Chemicals.** The antibodies were purchased as follows: the anti-TRIB3 was from Novus Biologicals (Littleton, CO, USA); the anti-DDIT4 and anti-TSC22D3 were from Proteintech (Chicago, IL, USA); the anti- $\beta$ -actin was from Santa Cruz Biotechnology (Santa Cruz, CA, USA), and anti- PCK2, anti-AKT1 and anti-phospho-AKT1 were from Cell Signaling Technology (Beverly, MA, USA). Commercially available nano-size gold particles were obtained from Sigma Aldrich (St. Louis, MO, USA) and evaluated by transmission electron microscopy (TEM). Prior to their addition to the culture medium, the gold nanoparticles (AuNPs) were dispersed in ultra-pure water (stock solution of 36  $\mu\text{g/ml}$ ) with sonication.

**Microarray Analysis.** Changes in gene expression in response to AuNP exposure were evaluated in A549 cells. The cells treatment and RNA preparation protocols were as previously described<sup>25</sup>. Briefly, cells were exposed to AuNPs for 24 h, total RNA was isolated using an RNeasy Mini Kit (Qiagen Inc., Valencia, CA, USA). The cDNA microarray analyses were conducted by the Phalanx Biotech Group (Hsinchu, Taiwan) using Human OneArray system of 32,050 60-mer sense-strand oligonucleotides corresponding to 30,968 human genome probes and 1,082 experimental control probes.

**Quantitative Real-time PCR (qPCR).** Total cellular RNAs were extracted using an RNeasy Mini Kit (Qiagen) according to the manufacturer's protocol. Single-stranded cDNA was synthesized from 2  $\mu\text{g}$  of RNA using an ImProm-II Reverse Transcriptase kit (Promega, Madison, WI, USA). Specific primers (Supplemental Table 1) were designed using the probe finder software from Roche Applied Science; this software, which is available online at the Universal ProbeLibrary Assay Design Center, is based on the Minimum Information for Publication of Quantitative Real-Time PCR Experiments (MIQE) Guidelines. Specific probes were selected from the Universal ProbeLibrary collection (Roche). The qPCR analysis was performed utilizing a LightCycler Nano (Roche). The results were normalized with respect to the expression of *TBP* and are presented as relative expression levels.

**Immunoblotting.** Cell extracts were prepared in lysis buffer (50 mM HEPES, pH 7.5, 150

mM NaCl, 5 mM EDTA, 1% Triton X-100, 50 mM NaF, 1 mM Na<sub>3</sub>VO<sub>4</sub>, 10% glycerol, and a protease inhibitor cocktail). Equal amounts of proteins were separated by sodium dodecyl sulfate-polyacrylamide gel electrophoresis (SDS-PAGE) and transferred to polyvinylidene difluoride (PVDF) membranes (Millipore, Billerica, MA, USA). The membranes were blocked, washed, probed with the indicated primary antibodies, washed again, and incubated with horseradish peroxidase-conjugated secondary antibodies for 1 h. Finally, the blots were washed, and then developed using enhanced chemiluminescence (ECL) reagents (Millipore) according to the manufacturer's protocol.

**Flow Cytometry.** Cells were trypsinized, washed once with PBS and fixed overnight in 70% ethanol. The fixed cells were washed twice with PBS, and then treated with RNase A and propidium iodine buffer for 30 min in the dark. Fluorescence activated cell sorting (FACS) was performed using a Cytomics FC500 Flow Cytometry (Beckman Coulter).

**Statistical Analyses.** All experiments were performed in triplicate, and the presented data represent the average of three replicate cultures. Standard deviations of the mean are indicated in the figures. The significances of between-group differences were determined using the Student's *t*-test. A *P*-value < 0.05 was considered to be statistically significant.

## Results

### cDNA Microarray Analysis and Comparison of Gene Expression Profiles

Commercially available AuNPs of three different particle sizes were used to perform genome-wide transcriptional profiling for AuNP exposure. Gene expression profiles were obtained using the Human OneArray system (Phalanx Biotech Group). Human A549 cells were exposed for 24 h to 39-nm, 41-nm, and 45-nm AuNPs at sublethal doses (IC<sub>50</sub>) that had been previously determined using MTS assays<sup>24</sup>. cDNA microarray analysis was then used to identify genes that were significantly (fold change >1.5; *P*<0.05 by *t*-test) induced by the tested AuNPs (Fig. 1A). We observed significant increases in the expression levels of 1763, 1642, and 1798 genes in A549 cells

treated with 39-, 41-, and 45-nm AuNPs, respectively (Fig. 1B). A total of 409 genes were commonly up-regulated in cells exposed to all three tested AuNPs. To identify potential biomarkers of AuNP exposure, we compared these 409 up-regulated genes to the 1654 genes previously shown to be up-regulated following exposure of MRC-5 cells to 41-nm AuNPs<sup>25</sup>. We identified 71 genes that were commonly up-regulated in AuNP-treated MRC-5 and A549 cells.

### **Identification and Validation of the Four Selected AuNP-induced Genes in Different Cell Lines**

From among the 71 commonly up-regulated genes, we selected the 30 most highly induced genes and subjected them to qPCR-based validation. Of them, nine were confirmed to be transcriptionally induced in A549 cells treated with all three tested AuNPs (data not shown). *TSC22D3*, *TRIB3*, *PCK2* and *DDIT4*, showed the highest sensitivities (fold change >3.5;  $P < 0.05$  by *t*-test) (Fig. 2A), and were thus selected as candidate biomarkers.

In addition to inhalation, humans may be exposed to NPs through other routes, including ingestion. In this case, the NPs might be absorbed into the circulation and ultimately distributed to various target organs, including the kidneys and liver. To test the potential cell-type specificity of our candidate biomarkers, we examined their AuNP-mediated up-regulation in two other human cell lines (HEK293 and HepG2). Indeed, *TSC22D3*, *TRIB3*, *PCK2* and *DDIT4* were all significantly up-regulated in HEK293 and HepG2 cells (Fig. 2B and C). Interestingly, *TSC22D3* expression was more strongly induced in A549 cells compared to HEK293 cells; *TRIB3* was more highly induced in HEK293 cells compared to HepG2 cells; *PCK2* was weakly induced in HepG2 cells compared to the other cell lines; and *DDIT4* was similarly up-regulated in all of the tested cell lines (Fig. 2). We then examined the ability of the four selected genes to discriminate between AuNP exposure and micro-Au or nano-TiO<sub>2</sub> exposure. Indeed, our qPCR analyses revealed that the same concentrations of micro-Au and nano-TiO<sub>2</sub> failed to up-regulate any of our candidate biomarkers in the tested cell lines (Fig. 2).

### **The Dose-Dependence of Candidate Biomarkers Induction Following AuNPs Treatment of the Different Cell Lines**

We then examine the dose-response characteristics of the four candidate biomarkers in the different cell lines following treatment with the three tested AuNPs. *TSC22D3* mRNA levels were robustly and dose-dependently induced in A549 and HepG2 cells following treatment with 39-, 41-, 45-nm AuNPs (Fig. 3A and C), whereas weaker dose-dependent responses were noted in HEK293 cells (Fig. 3B). Among the tested AuNPs, the 45-nm AuNPs exhibited a weaker ability to induce *TSC22D3* expression in A549 and HepG2 cells (Fig. 3A and C). *TRIB3* was dose-dependently induced by the tested AuNPs in all three cell lines, with the strongest and weakest inductions observed in AuNP-treated HEK293 and HepG2 cells, respectively (Fig. 4). *PCK2* was dose-dependently induced in all three cell lines following AuNP treatment, with weaker induction seen in HepG2 cells (for all three particle sizes) (Fig. 5). Notably, the AuNP-induced up-regulation of *DDIT4* was similar and dose-dependent in all tested cell lines regardless of the particle size (Fig. 6). Overall, A549 cells tended to react more strongly to AuNP exposure, whereas HepG2 cells tended to be less sensitive to AuNP-treatment. The three tested AuNPs also up-regulated the four selected genes in AGS cells (a gastric adenocarcinoma cell line) (Supplemental Fig. S1).

### **Protein Levels of the Candidate Biomarkers Following AuNP Treatment of A549 Cells**

We used immunoblot analysis to elucidate the protein levels of the candidate biomarkers in AuNP-treated A549 cells, and found that *TSC22D3*, *TRIB3*, *PCK2* and *DDIT4* were dose-dependently elevated by the three tested AuNPs (Fig. 7A), but not by the same concentrations of micro-Au or nano-TiO<sub>2</sub> (Fig. 7B). Moreover, co-treatment of cells with AuNPs plus micro-Au or nano-TiO<sub>2</sub> did not alter the AuNP-induced up-regulations of the candidate biomarker proteins (Fig. 7C). Based on these findings, we further investigated some downstream effects of *TRIB3* and *DDIT4*. Consistent with a previous reports that *TRIB3* negatively regulates the phosphorylation and activation of AKT (a serine/threonine kinase involved in cell proliferation and growth)<sup>26</sup>, we found that the

activated form of AKT was significantly and dose-dependently down-regulated in cells treated with AuNP (Fig. 7A), but not micro-Au or nano-TiO<sub>2</sub> (Fig. 7B and C). Our analysis of cell cycle progression revealed that AuNP-treated cells accumulated in the G1 and G2/M phases (Fig. 7D), suggesting that the AuNP-mediated induction of DDIT4 triggered alterations in cell cycle progression.

### **Benzo[α]pyrene Fails to Up-regulate the Candidate Biomarkers**

To test whether the candidate biomarkers could respond to other stress conditions, we examined their levels in cells treated with benzo[α]pyrene. This polycyclic aromatic hydrocarbon (PAH) compound, which is often found in combustion products (e.g., cigarette smoke and industrial combustion reactions), is metabolically activated in cells to yield several genotoxic compounds. However, as shown in Figure 8, benzo[α]pyrene treatment did not modulate the expression levels of the candidate biomarkers in A549 cells under our experimental conditions, providing additional evidence that the identified gene signature may be specific to AuNP exposure.

### **Characterization of the tested AuNPs**

We previously evaluated the three tested AuNPs by TEM<sup>24</sup>. To further characterize the tested AuNPs, we used sonication to disperse them in water, and applied Laser Doppler Velocimetry (LDV; Malvern Zetasizer NanoZS Instruments, Worcestershire, UK) to characterize their zeta potentials. As shown in Figure 9A, the average zeta potentials of the 39-, 41- and 45-nm AuNPs in water were 59.4, 64, and 63.3 mV, respectively. Furthermore (and consistent with the data provided by Sigma-Aldrich), our UV spectral analysis (HITACHI U4100 spectrophotometer, Japan) revealed that the absorption wavelengths of the 39-, 41- and 45-nm AuNPs were 783, 805, and 831 nm, respectively (Fig. 9B).

Based on the above-described data, we conclude that the tested AuNPs can up-regulate the expression levels of *TSC22D3*, *TRIB3*, *PCK2* and *DDIT4* in a non-cell-type-specific manner,

suggesting that elevated levels of these transcripts might be indicative of AuNP exposure. Although we are still at the early stages of defining and implementing specific biomarkers in the field of nanotechnology, our data indicate that it may be possible to define reliable diagnostic and predictive biomarkers for nano-material exposure.

## Discussion

It is important to identify biomarkers and evaluate their potential ability to predict the clinical responses of a given patient. In the assessment of Alzheimer's disease, for example, biomarkers have been integrated into the diagnostic schemes recommended by the International Work Group (IWG), the National Institute on Aging (NIA) and the Alzheimer's Association (AA)<sup>27</sup>. Physical and chemical stress can alter the gene transcription profiles of cells, such that molecular signatures can act as diagnostic tools for detecting toxicant exposure<sup>28,29</sup>. Molecular signatures can be also be used to prioritize screening for environmental toxicant exposures, potentially minimizing the use of animals and the cost/time required for such studies<sup>30</sup>. Because there are few known biomarkers for the susceptibility to nano-material exposure, additional candidate gene signatures must be examined. Here, we identified four novel potential biomarker genes (*TSC22D3*, *PCK2*, *TRIB3* and *DDIT4*) that were significantly up-regulated following the exposure of different cell lines to three different sizes of AuNPs at identical doses and exposure times. Conversely, the inductions of the four potential biomarker genes were significantly attenuated following removal of the tested AuNPs (Supplemental Fig. S2). Thus, the AuNP-induced up-regulation of *TSC22D3*, *PCK2*, *TRIB3* and *DDIT4* appears to be a gene signature that is shared by four cell lines (A549, HEK293, HepG2 and AGS cells) representing the common routes of NP exposure and metabolism.

NPs usually enter the body via inhalation or ingestion, and are subsequently circulated to target organs, such as the kidneys and liver. Once NPs have been taken up by cells, they might interact with internal or membrane molecules, damaging intracellular molecules and inducing stress responses. Based on the expression levels of the selected marker genes in cultured cells, we speculate that liver

cells may be less sensitive to AuNP exposure compared to the other tested cell types. This result indicates that different exposure routes may target cells that differ in their sensitivity to NP. Our findings also suggest that our system may be used for the quantitative assessment of nano-material exposure, and emphasize the importance of identifying unbiased biomarkers for the characterization of NP responses. Future work is warranted to examine the dose-response characteristics of the identified-four-gene signature, its potential downstream biological significance, and its relevance to human NP exposure.

Of the proteins encoded by our candidate biomarkers, TRIB3 was found to be induced under conditions of cell stress<sup>31</sup>, but there is some controversy regarding whether it has anti-apoptotic or pro-apoptotic function in stressed cells<sup>32,33</sup>. The activation of TRIB3 mRNA and protein levels observed in the present work is therefore indicative of a stress response in AuNP-exposed cells. *PCK2*, in contrast, is a nuclear gene that encodes mitochondrial phosphoenolpyruvate carboxylase (PEPCK-M). This protein plays a critical role by decarboxylating oxaloacetate (OAA) to phosphoenolpyruvate (PEP); notably the synthesis of PEP is important for insulin secretion, gluconeogenesis and the tricarboxylic acid cycle (TCA) flux<sup>34,35</sup>. PEPCK-M activity is also present in non-gluconeogenic tissues, where it appears to modulate cell survival under various stress situations, such as nutrient restriction and ER stress<sup>36</sup>. Notably, the gene expression levels of *TRIB3* and *PCK2* are known to be closely related, and TRIB3 appears to be involved in regulating the expression of *PCK2*<sup>37</sup>. *TSC22D3* encodes the glucocorticoid-induced leucine zipper (GILZ, TSC22D3) protein, which was originally identified during a systematic study of genes that were transcriptionally induced by glucocorticoids (GCs) and appeared to be responsible for GC-activated apoptosis<sup>38,39</sup>. Subsequently, TSC22D3 was shown to mediate several GC-independent functions (e.g., inflammation, cell cycle progression, apoptosis and differentiation) depending on the cell type and involved binding partners<sup>40</sup>. *DDIT4* (also known as *RTP801*, *REDD1* and *Dig-1*) is a stress-response gene that was first identified as being up-regulated in response to hypoxia and DNA damage<sup>41,42</sup>. It negatively regulates mTORC1 to reduce protein synthesis, and is an important

modulator of the cellular response to a variety of stress situations<sup>43</sup>. The observed activation of DDIT4 suggests that AuNP exposure triggers the DNA damage response, causing cells to activate their cell cycle checkpoints and DNA repair mechanisms. This conclusion is consistent with the findings of our previous studies<sup>24, 25</sup>. Moreover, in previous studies, we have examined the cytotoxicity of various concentrations of all three AuNPs in the tested cell lines over a 3-day treatment<sup>24, 25</sup> (compared to the 24-h treatment period used in the above-described experiments). Thus, the gene signature identified herein may be detectable before significant toxicity is exerted, thereby reflecting early exposure to AuNPs. These biomarkers could potentially be translated into clinical practice for the assessment of NP exposure in the absence of overt symptoms.

## Conclusion

Correlative studies with human cell lines and functional experiments in animals have linked NP exposure with cytotoxicity. The identification of reliable biomarkers could greatly facilitate the development of clinical strategies for the early diagnosis of nano-material exposure in humans. In the present study, we identified four novel and reliable gene biomarkers for AuNP exposure, and show that their up-regulation is shared among AuNP-treated A549, HEK293, HepG2 and AGS cells. These gene responses in different cell types suggests that it might be possible to construct a compact panel of readouts to assess the responses of various target cell types to certain NPs. The present work and our previous studies combine to describe an approach for the assessing NP-derived responses, through dye-free, real-time screening of cytotoxicity<sup>24</sup> followed by genome-wide gene expression profiling<sup>25</sup> and identification of a specific NP-related gene signature (this paper). Further studies will be needed to establish the full clinical utility of the identified biomarkers. Given the numerous variables inherent to field monitoring (e.g., the presence of air pollutants and particulate matters), it is not yet clear whether the identified four-gene signature will successfully reflect AuNP exposure when applied to environmental screening. To boost the signal-to-noise and specificity of such testing, researchers must continue to seek promising NP-specific biomarkers and sensitive screening

strategies that exclude interference from non-target components. However, the four-gene signature identified herein could potentially act as a biomarker for AuNP exposure and dose responsiveness, and might be integrated into human health risk assessment in the future.

### **Acknowledgements**

Financial support was provided by grants from the Environmental Analysis Lab, Environmental Protection Administration, Executive Yuan, Taiwan (EPA-102-1605-02-01 and EPA-103-1605-02-01)

### **Authors' contributions**

RYL carried out the mRNA preparation for cDNA microarray analysis, comprehensive gene expression profiles and Realtime PCR experiments; XT and HFT performed the Western blot analyses; YSY characterized zeta potentials of the AuNPs; PJC consulted on the primary study; SMC conceived the study, participated in the study design and coordination, and contributed to the writing, review, and revision of the manuscript. All authors read and approved the final manuscript.

### **Conflict of interest**

None of the authors reports any conflict of interest or other relationship or activity that could appear to have influenced the submitted work.

### **Figure legends:**

**Fig. 1** (A) Hierarchical cluster visualization and heatmap of genes found to be differentially expressed in AuNP-treated A549 cells, clustered with correlation distance and complete linkages. (B) Venn diagram of the genes that were significantly up-regulated in A549 cells exposed to sublethal doses of three different sized of AuNPs for 24 h. The numbers in the figure represent the genes that were up-regulated by  $> 1.5$ -fold by each of the tested AuNPs compared to untreated control cells. A

total of 409 genes were commonly up-regulated; these were further compared to the 1654 genes previously reported to be up-regulated in MRC-5 cells treated with 41-nm AuNPs<sup>25</sup>. Of the 71 genes up-regulated in both cell lines following AuNP treatment, the 30 top ranked genes based on magnitude of induction were further evaluated by quantitative real-time PCR (qPCR) analyses.

**Fig. 2** Quantitative real-time PCR of *TSC22D3*, *TRIB3*, *PCK2* and *DDIT4* in different cell lines. (A) A549 (B) HEK293 and (C) HepG2 cells were exposed to 360 ng/ml AuNPs, micro-Au or nano-TiO<sub>2</sub> for 24 h, and then the mRNA levels of these four genes were determined by qPCR. \* $P < 0.05$ ; and \*\* $P < 0.01$ .

**Fig. 3** Dose-dependent induction of *TSC22D3* by the three tested AuNPs. (A) A549, (B) HEK293 and (C) HepG2 cells were exposed to 0, 72, 180 and 360 ng/ml AuNPs for 24 h, and the mRNA levels of *TSC22D3* were determined by qPCR. \* $P < 0.05$ ; and \*\* $P < 0.01$ .

**Fig. 4** Dose-dependent induction of *TRIB3* by the three tested AuNPs. (A) A549, (B) HEK293 and (C) HepG2 cells were exposed to 0, 72, 180 and 360 ng/ml AuNPs for 24 h, and the mRNA levels of *TRIB3* were determined by qPCR. \* $P < 0.05$ ; and \*\* $P < 0.01$ .

**Fig. 5** Dose-dependent induction of *PCK2* by the three tested AuNPs. (A) A549, (B) HEK293 and (C) HepG2 cells were exposed to 0, 72, 180 and 360 ng/ml AuNPs for 24 h, and the mRNA levels of *PCK2* were determined by qPCR. \* $P < 0.05$ ; and \*\* $P < 0.01$ .

**Fig. 6** Dose-dependent induction of *DDIT4* by the three tested AuNPs. (A) A549, (B) HEK293 and (C) HepG2 cells were exposed to 0, 72, 180 and 360 ng/ml AuNPs for 24 h, and the mRNA levels of *DDIT4* were determined by qPCR. \* $P < 0.05$ ; and \*\* $P < 0.01$ .

**Fig. 7** Immunoblotting analyses of the selected genes in A549 cells. (A) A549 cells were treated with 0-360 ng/ml AuNPs for 24 h, and protein levels were determined by immunoblotting using antibodies specific against TSC22D3, TRIB3, PCK2, DDIT4, phosphor-AKT (pS473) and AKT. Beta-actin was used as the internal control. (B) A549 cells were treated with 360 ng/ml of 39-, 41-, or 45-nm AuNPs, micro-Au, or nano-TiO<sub>2</sub> for 24 h, and protein levels were determined as described in panel (A). (C) A549 cells were treated with 360 ng/ml of 41-nm AuNPs in the presence or absence of 360 ng/ml micro-Au or nano-TiO<sub>2</sub> for 24 h, and protein levels were determined as described in panel (A). (D) A549 cells were treated with 360 ng/ml of 41-nm AuNPs at for 24 h, and cell cycle progression was evaluated by flow cytometry.

**Fig. 8** Benzo[ $\alpha$ ]pyrene does not induce the expression of the four selected genes in A549 cells. (A) A549 cells were exposed to different doses of benzo[ $\alpha$ ]pyrene for 3 days and cell viability was measured by WST1 assay (Roche). (B) Cells were treated with 40  $\mu$ M benzo[ $\alpha$ ]pyrene for 24 h, and the mRNA levels of *TSC22D3*, *TRIB3*, *PCK2* and *DDIT4* were determined by qPCR. Abbreviation: N.S., not significant.

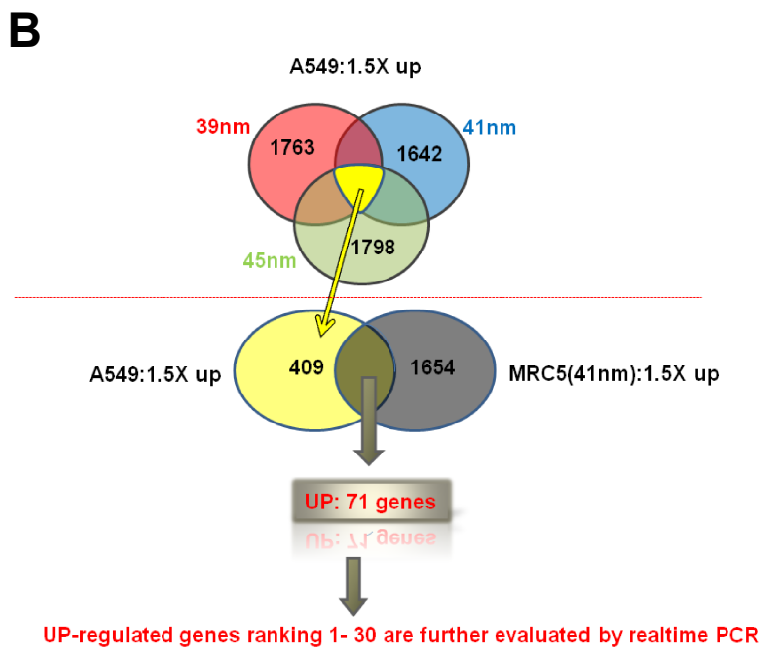
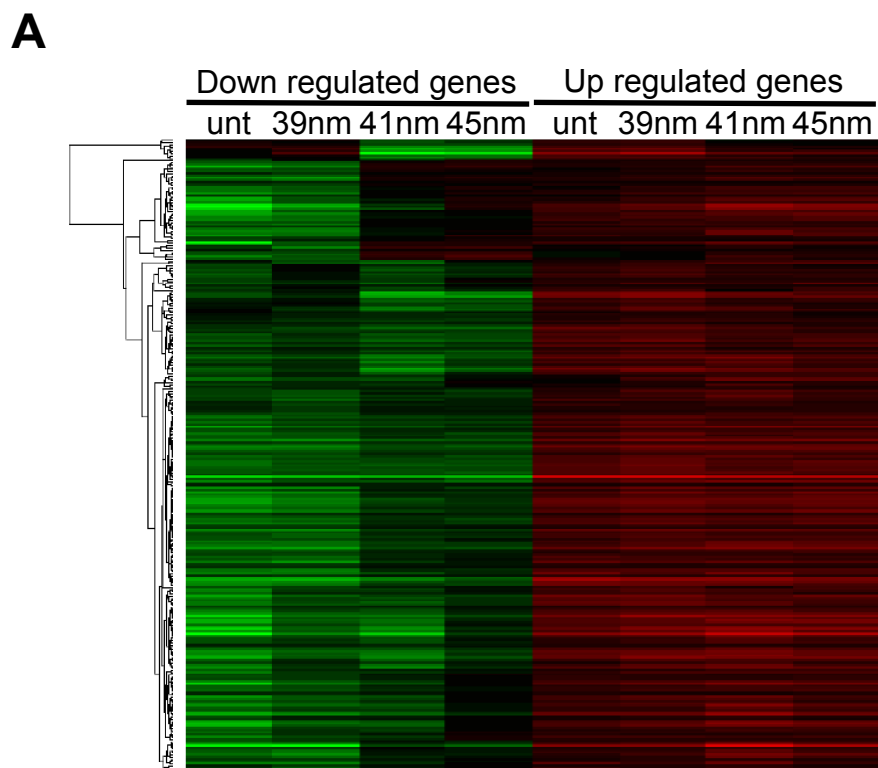
**Fig. 9** Characterization of AuNPs. (A) Zeta-potentials of AuNPs suspended in deionized water. (B) UV spectra of AuNPs.

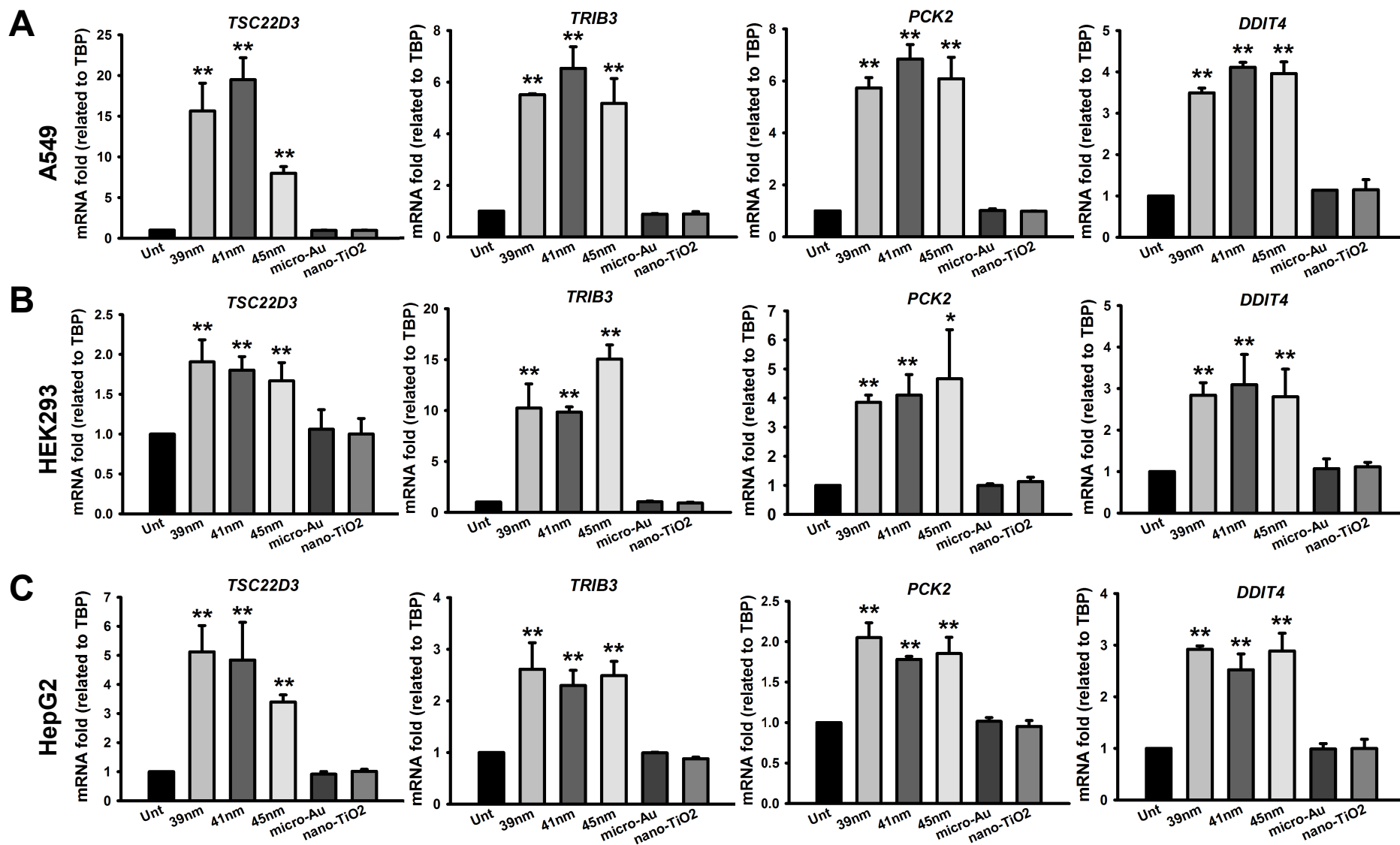
#### REFERENCES:

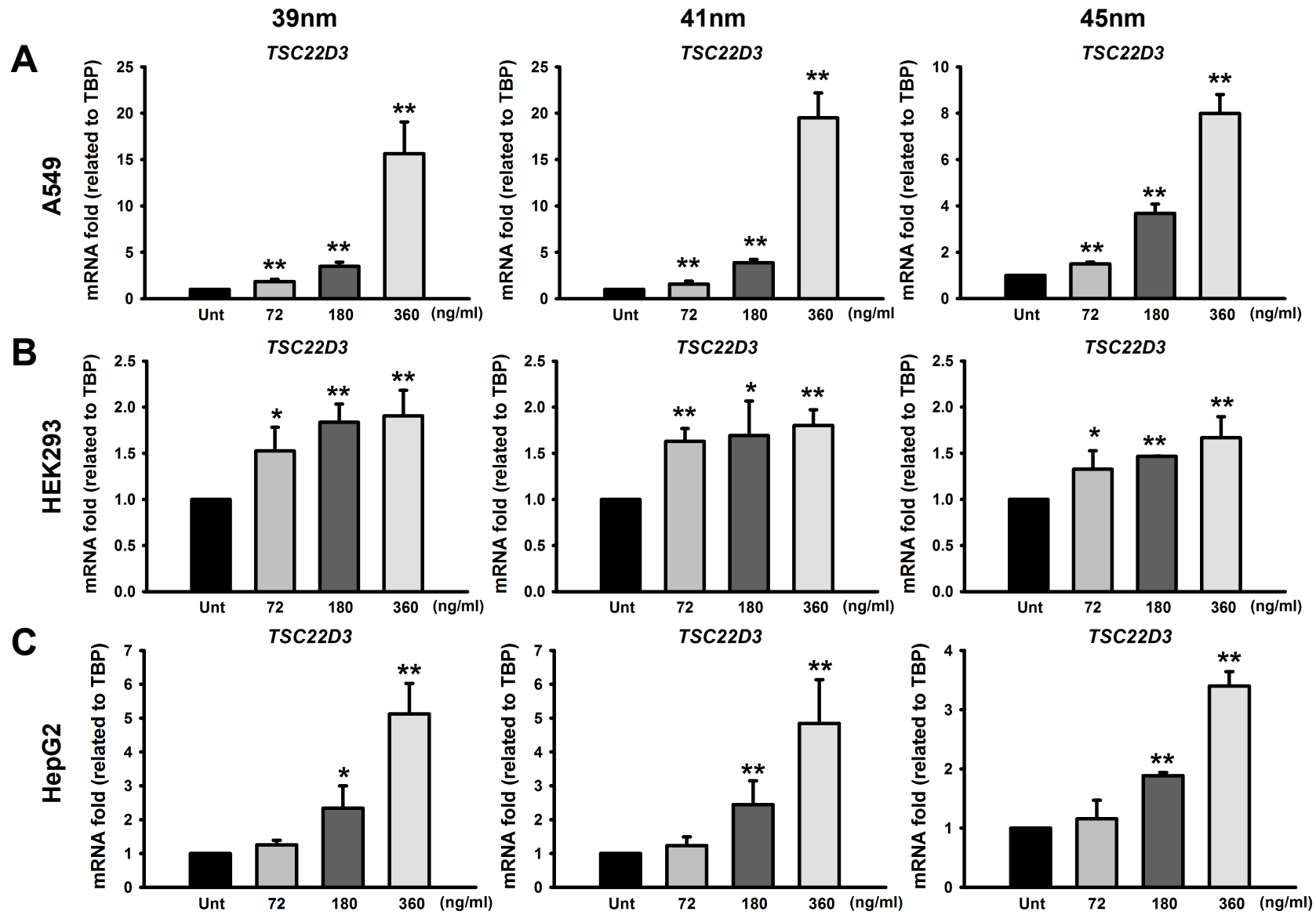
1. L. Dykman and N. Khlebtsov, *Chem Soc Rev*, 2012, 41, 2256-2282.
2. A. M. Knaapen, P. J. Borm, C. Albrecht and R. P. Schins, *Int J Cancer*, 2004, 109, 799-809.
3. P. J. Borm, R. P. Schins and C. Albrecht, *Int J Cancer*, 2004, 110, 3-14.
4. S. W. Kim, J. I. Kwak and Y. J. An, *Environ Sci Technol*, 2013, 47, 5393-5399.
5. K. T. Kim, T. Zaikova, J. E. Hutchison and R. L. Tanguay, *Toxicol Sci*, 2013, 133, 275-288.
6. S. Hussain, J. A. Vanoirbeek, S. Haenen, V. Haufroid, S. Boland, F. Marano, B. Nemery and P. H. Hoet, *Biomed Res Int*, 2013, 2013, 923475.
7. H. Chen, A. Dorrigan, S. Saad, D. J. Hare, M. B. Cortie and S. M. Valenzuela, *PLoS One*, 2013,

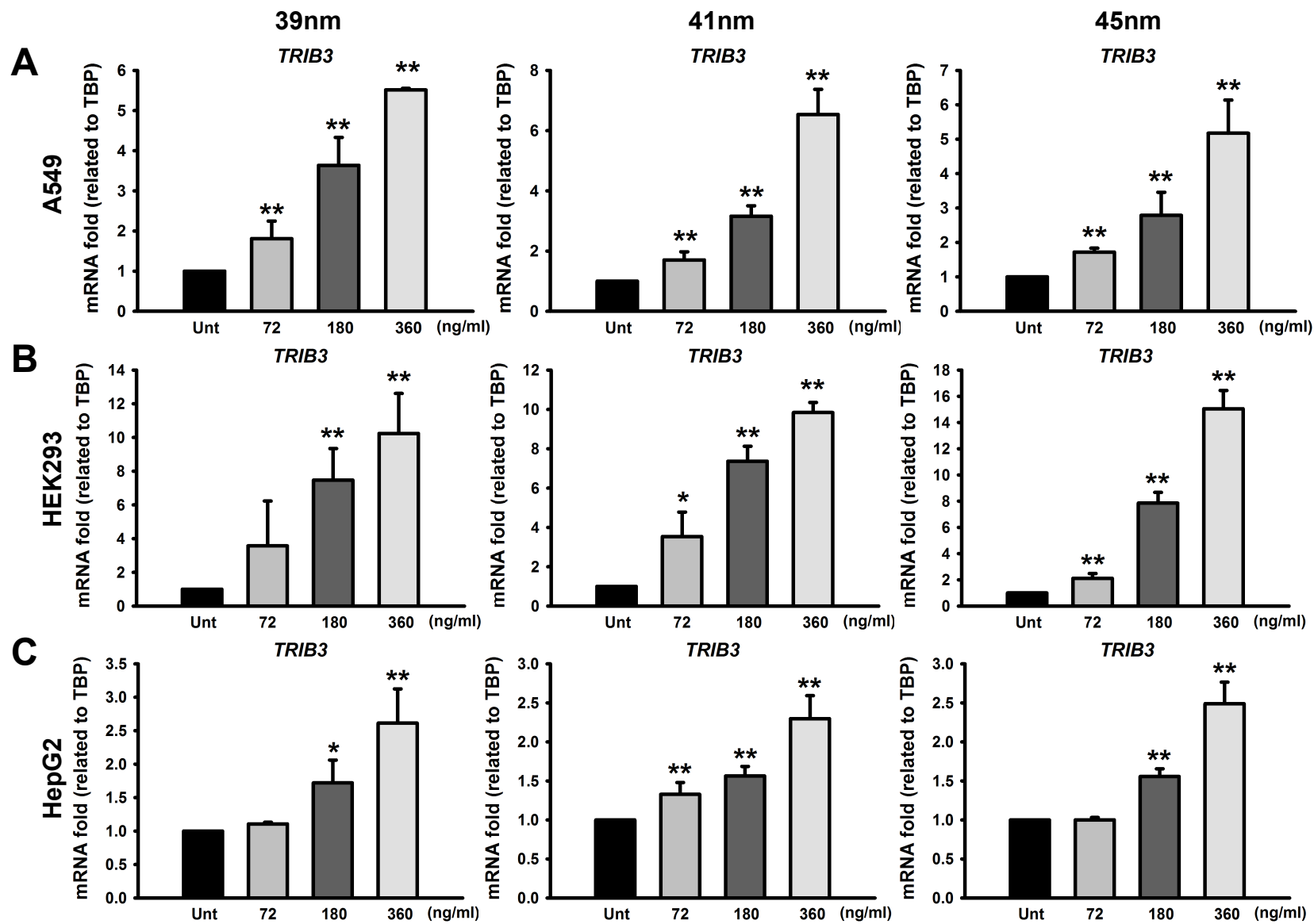
- 8, e58208.
8. S. Tuomela, R. Autio, T. Buerki-Thurnherr, O. Arslan, A. Kunzmann, B. Andersson-Willman, P. Wick, S. Mathur, A. Scheynius, H. F. Krug, B. Fadeel and R. Lahesmaa, *PLoS One*, 2013, 8, e68415.
  9. J. A. Bourdon, A. Williams, B. Kuo, I. Moffat, P. A. White, S. Halappanavar, U. Vogel, H. Wallin and C. L. Yauk, *Toxicology*, 2013, 303, 83-93.
  10. R. G. Gray, P. Quirke, K. Handley, M. Lopatin, L. Magill, F. L. Baehner, C. Beaumont, K. M. Clark-Langone, C. N. Yoshizawa, M. Lee, D. Watson, S. Shak and D. J. Kerr, *J Clin Oncol*, 2011, 29, 4611-4619.
  11. S. Kraus, I. Nabiochtchikov, S. Shapira and N. Arber, *Cancer Lett*, 2014, 347, 15-21.
  12. V. S. Wilson, N. Keshava, S. Hester, D. Segal, W. Chiu, C. M. Thompson and S. Y. Euling, *Toxicol Appl Pharmacol*, 2011, 271, 299-308.
  13. S. Y. Euling, L. D. White, A. S. Kim, B. Sen, V. S. Wilson, C. Keshava, N. Keshava, S. Hester, M. A. Ovacik, M. G. Ierapetritou, I. P. Androulakis and K. W. Gaido, *Toxicol Appl Pharmacol*, 2011, 271, 349-362.
  14. A. S. Kienhuis, J. G. Bessems, J. L. Pennings, M. Driessen, M. Luijten, J. H. van Delft, A. A. Peijnenburg and L. T. van der Ven, *Toxicol Appl Pharmacol*, 2011, 250, 96-107.
  15. M. B. Genter, D. M. Burman, S. Vijayakumar, C. L. Ebert and B. J. Aronow, *Physiol Genomics*, 2002, 12, 35-45.
  16. B. Sen, A. Wang, S. D. Hester, J. L. Robertson and D. C. Wolf, *Toxicology*, 2005, 215, 214-226.
  17. L. Peng, A. J. Barczak, R. A. Barbeau, Y. Xiao, T. J. LaTempa, C. A. Grimes and T. A. Desai, *Nano Lett*, 2010, 10, 143-148.
  18. L. Sheng, L. Wang, X. Sang, X. Zhao, J. Hong, S. Cheng, X. Yu, D. Liu, B. Xu, R. Hu, Q. Sun, J. Cheng, Z. Cheng, S. Gui and F. Hong, *J Hazard Mater*, 2014, 278C, 180-188.
  19. B. Li, Y. Ze, Q. Sun, T. Zhang, X. Sang, Y. Cui, X. Wang, S. Gui, D. Tan, M. Zhu, X. Zhao, L. Sheng, L. Wang, F. Hong and M. Tang, *PLoS One*, 2013, 8, e55563.
  20. G. Wang, R. K. Kelley and Gappnet, *PLoS Curr*, 2010, 2.
  21. S. Schubbert, K. Shannon and G. Bollag, *Nat Rev Cancer*, 2007, 7, 295-308.
  22. D. F. Hayes, R. C. Bast, C. E. Desch, H. Fritsche, Jr., N. E. Kemeny, J. M. Jessup, G. Y. Locker, J. S. Macdonald, R. G. Mennel, L. Norton, P. Ravdin, S. Taube and R. J. Winn, *J Natl Cancer Inst*, 1996, 88, 1456-1466.
  23. R. M. Simon, S. Paik and D. F. Hayes, *J Natl Cancer Inst*, 2009, 101, 1446-1452.
  24. S. M. Chuang, Y. H. Lee, R. Y. Liang, G. D. Roam, Z. M. Zeng, H. F. Tu, S. K. Wang and P. J. Chueh, *Biochim Biophys Acta*, 2013, 1830, 4960-4973.
  25. P. J. Chueh, R. Y. Liang, Y. H. Lee, Z. M. Zeng and S. M. Chuang, *J Hazard Mater*, 2014, 264C, 303-312.
  26. K. Du, S. Herzig, R. N. Kulkarni and M. Montminy, *Science*, 2003, 300, 1574-1577.

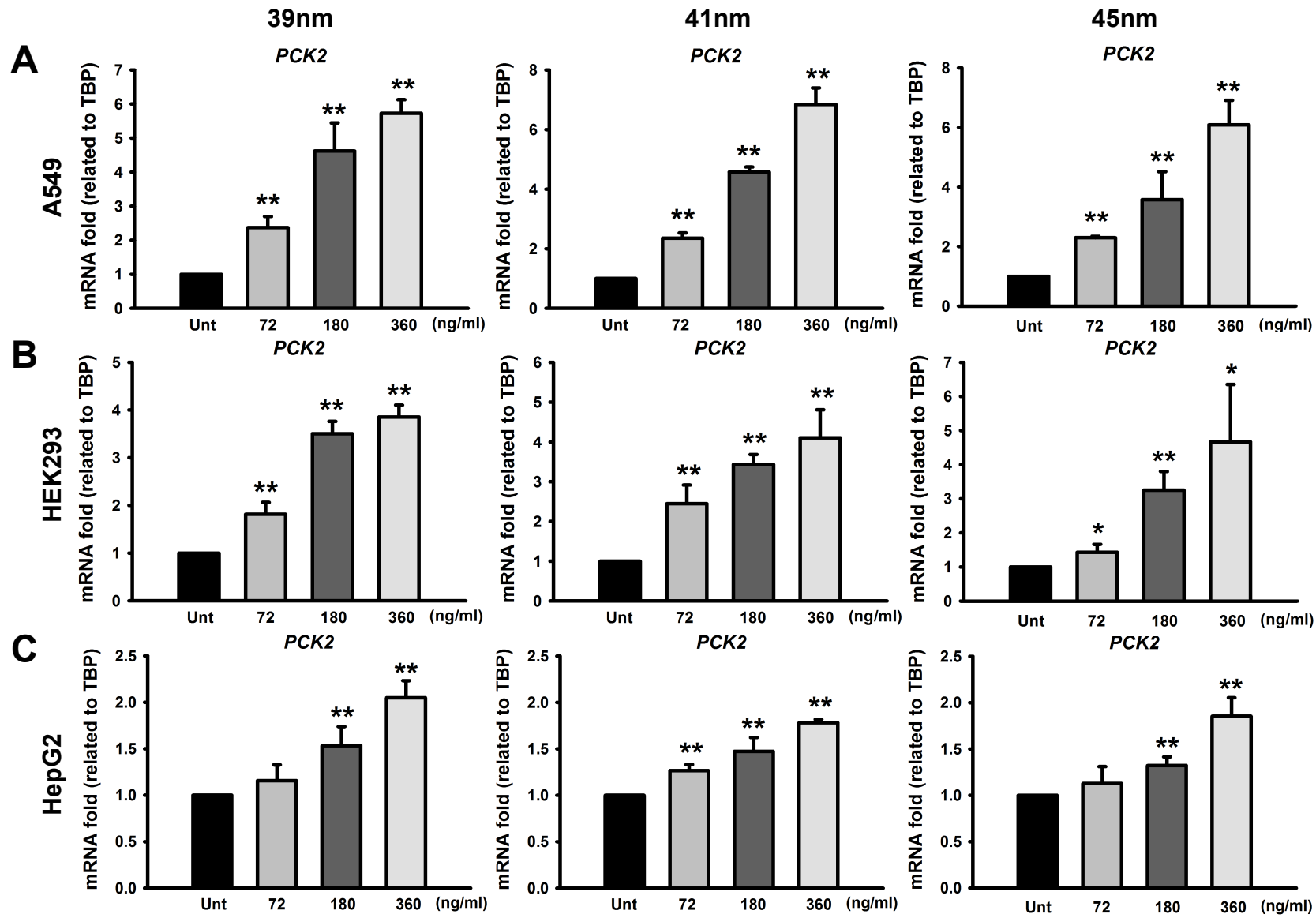
27. H. Hampel, S. Lista, S. J. Teipel, F. Garaci, R. Nistico, K. Blennow, H. Zetterberg, L. Bertram, C. Duyckaerts, H. Bakardjian, A. Drzezga, O. Colliot, S. Epelbaum, K. Broich, S. Lehericy, A. Brice, Z. S. Khachaturian, P. S. Aisen and B. Dubois, *Biochem Pharmacol*, 2014, 88, 426-449.
28. S. S. Auerbach, R. R. Shah, D. Mav, C. S. Smith, N. J. Walker, M. K. Vallant, G. A. Boorman and R. D. Irwin, *Toxicol Appl Pharmacol*, 2010, 243, 300-314.
29. M. R. Fielden, A. Adai, R. T. Dunn, 2nd, A. Olaharski, G. Searfoss, J. Sina, J. Aubrecht, E. Boitier, P. Nioi, S. Auerbach, D. Jacobson-Kram, N. Raghavan, Y. Yang, A. Kincaid, J. Sherlock, S. J. Chen and B. Car, *Toxicol Sci*, 2011, 124, 54-74.
30. D. J. Dix, K. A. Houck, M. T. Martin, A. M. Richard, R. W. Setzer and R. J. Kavlock, *Toxicol Sci*, 2007, 95, 5-12.
31. D. Ord and T. Ord, *Biochem Biophys Res Commun*, 2005, 330, 210-218.
32. N. Ohoka, S. Yoshii, T. Hattori, K. Onozaki and H. Hayashi, *EMBO J*, 2005, 24, 1243-1255.
33. K. Shimizu, S. Takahama, Y. Endo and T. Sawasaki, *PLoS One*, 2012, 7, e42721.
34. R. Stark, F. Guebre-Egziabher, X. Zhao, C. Feriod, J. Dong, T. C. Alves, S. Ioja, R. L. Pongratz, S. Bhanot, M. Roden, G. W. Cline, G. I. Shulman and R. G. Kibbey, *J Biol Chem*, 2014, 289, 7257-7263.
35. R. Stark and R. G. Kibbey, *Biochim Biophys Acta*, 2014, 1840, 1313-1330.
36. A. Mendez-Lucas, P. Hyrossova, L. Novellademunt, F. Vinals and J. C. Perales, *J Biol Chem*, 2014, 289, 22090-22102.
37. H. Oberkofler, A. Pfeifenberger, S. Soyol, T. Felder, P. Hahne, K. Miller, F. Krempler and W. Patsch, *Diabetologia*, 2010, 53, 1971-1975.
38. F. D'Adamio, O. Zollo, R. Moraca, E. Ayroldi, S. Bruscoli, A. Bartoli, L. Cannarile, G. Migliorati and C. Riccardi, *Immunity*, 1997, 7, 803-812.
39. M. Shibanuma, T. Kuroki and K. Nose, *J Biol Chem*, 1992, 267, 10219-10224.
40. E. Ayroldi and C. Riccardi, *FASEB J*, 2009, 23, 3649-3658.
41. T. Shoshani, A. Faerman, I. Mett, E. Zelin, T. Tenne, S. Gorodin, Y. Moshel, S. Elbaz, A. Budanov, A. Chajut, H. Kalinski, I. Kamer, A. Rozen, O. Mor, E. Keshet, D. Leshkowitz, P. Einat, R. Skaliter and E. Feinstein, *Mol Cell Biol*, 2002, 22, 2283-2293.
42. L. W. Ellisen, K. D. Ramsayer, C. M. Johannessen, A. Yang, H. Beppu, K. Minda, J. D. Oliner, F. McKeon and D. A. Haber, *Mol Cell*, 2002, 10, 995-1005.
43. J. Brugarolas, K. Lei, R. L. Hurley, B. D. Manning, J. H. Reiling, E. Hafen, L. A. Witters, L. W. Ellisen and W. G. Kaelin, Jr., *Genes Dev*, 2004, 18, 2893-2904.

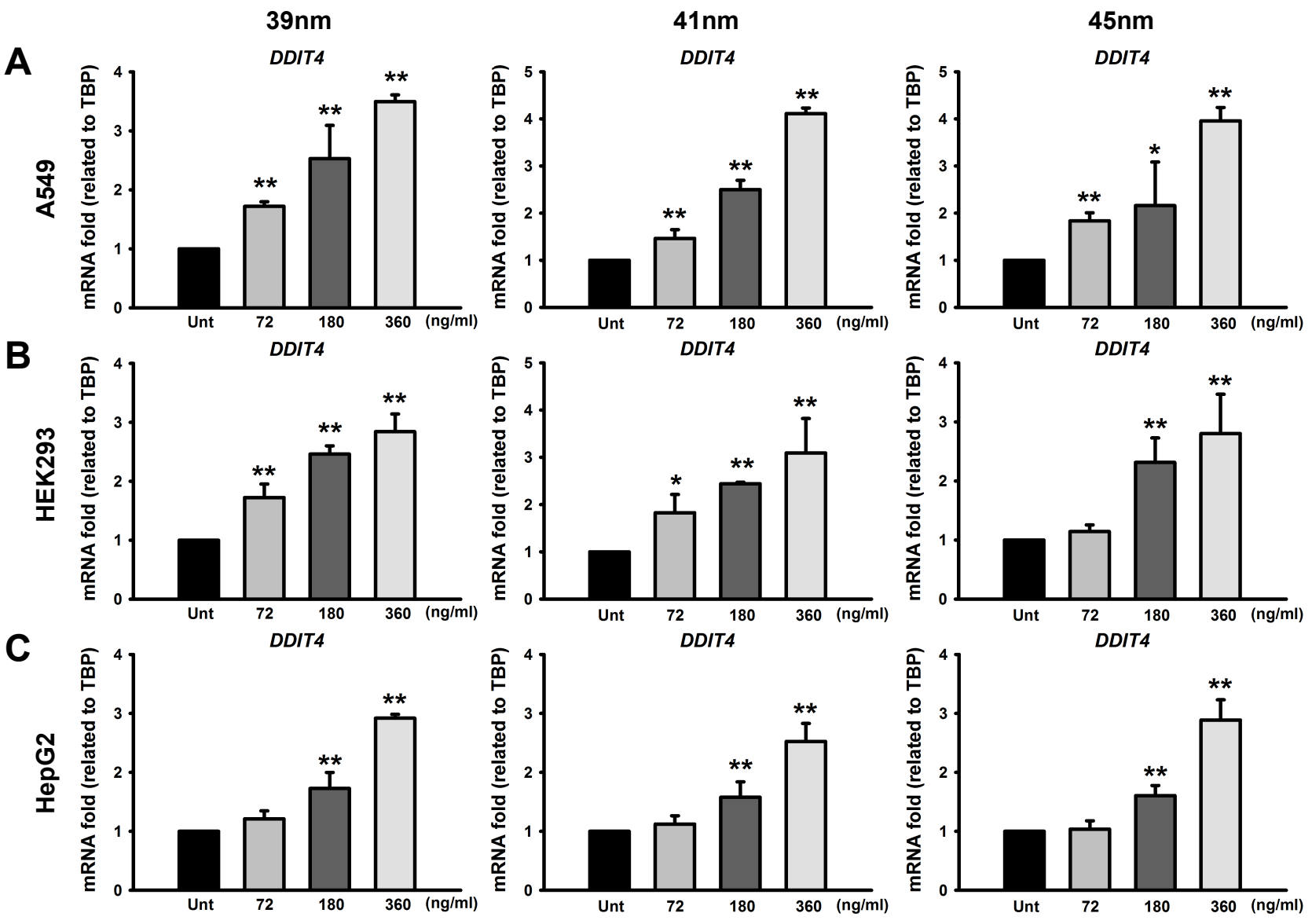


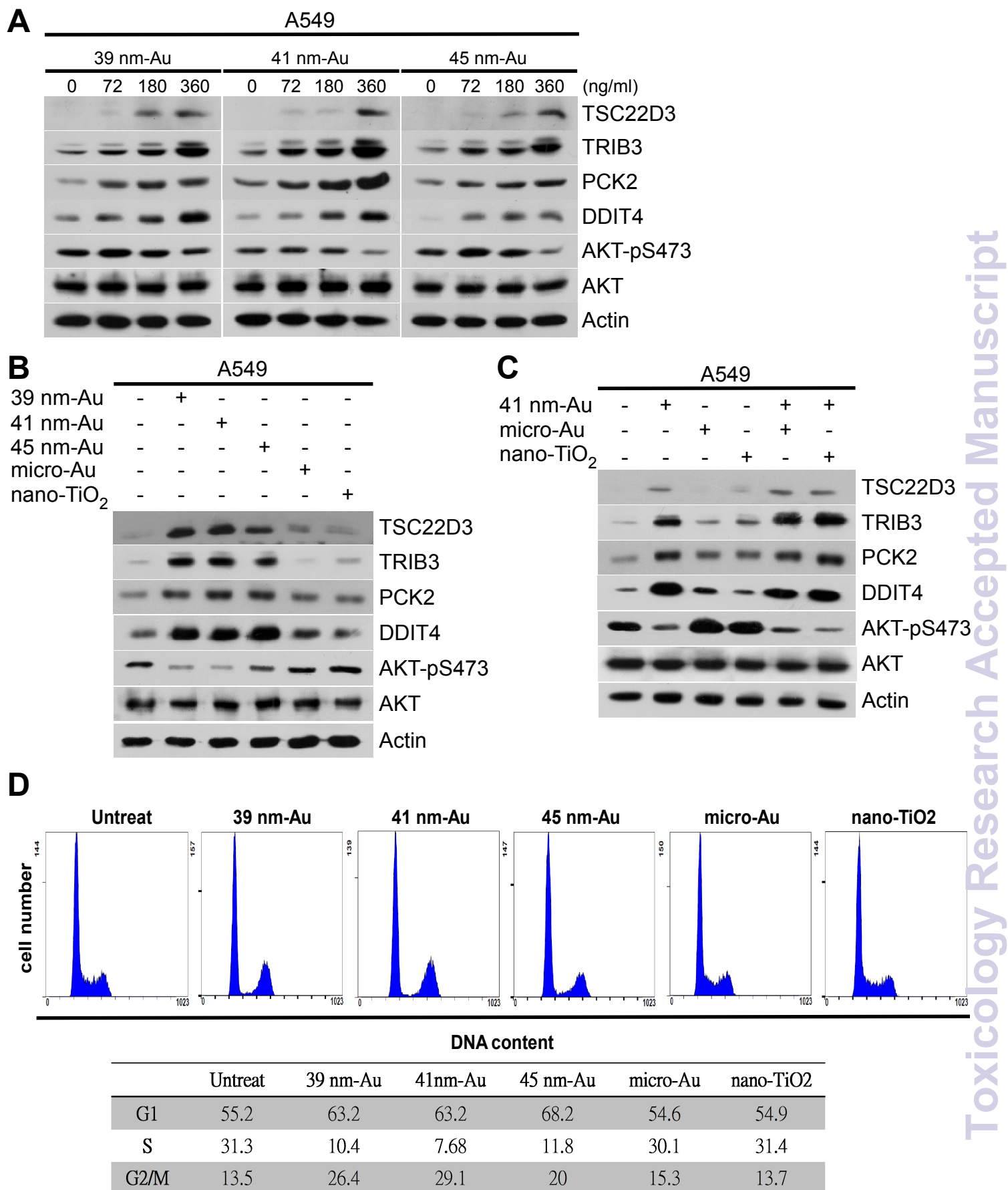












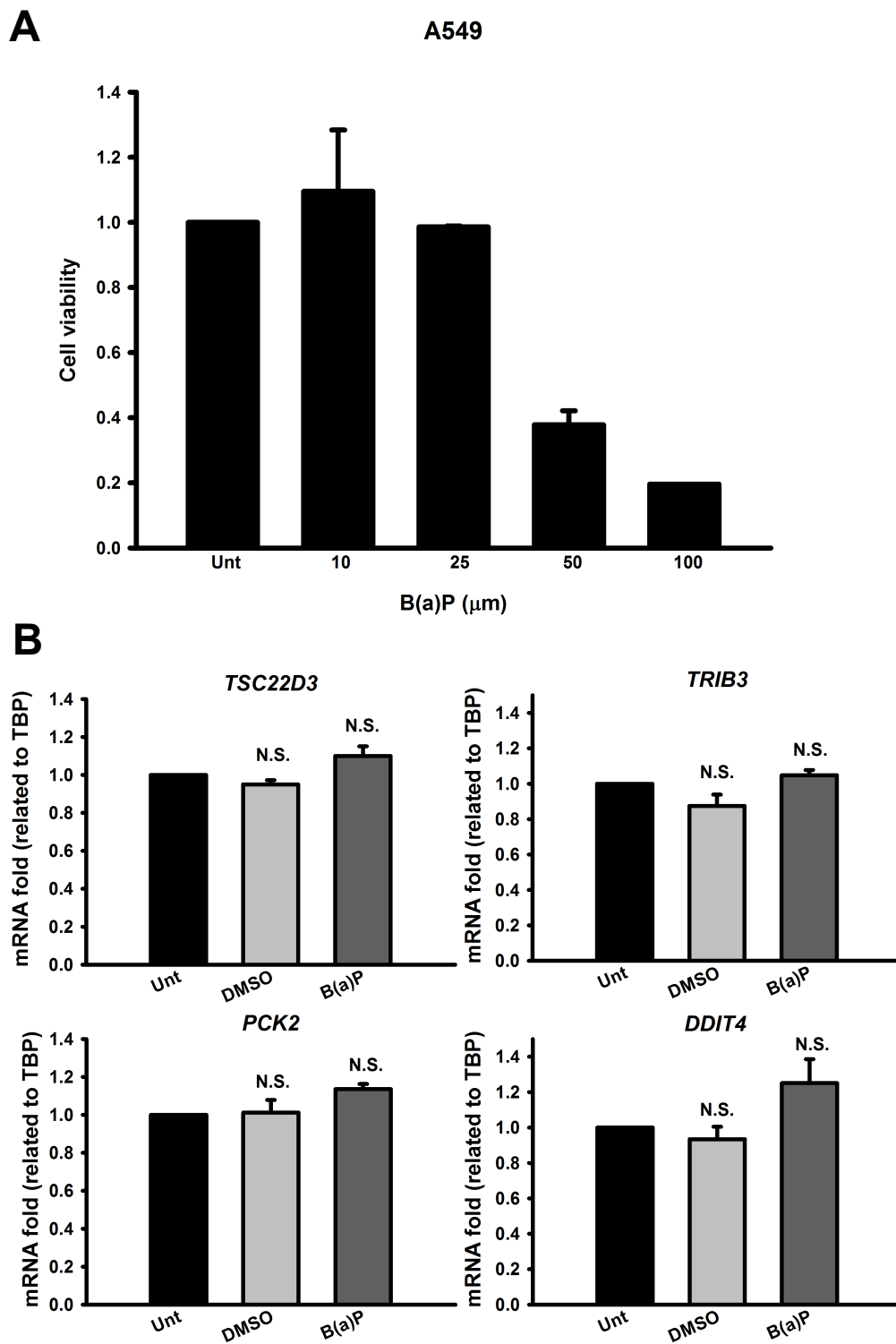
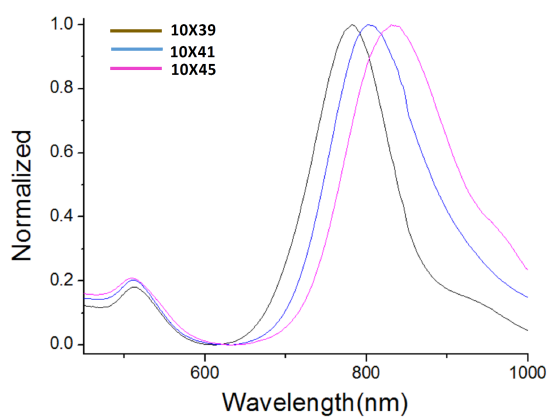


Figure 9

**A**

| AuNPs   | Zeta Potential (mV) | Zeta Deviation (mV) | Conductivity (mS/cm) |
|---------|---------------------|---------------------|----------------------|
| Au-39nm | 59.4                | 16.7                | 0.0639               |
| Au-41nm | 64.0                | 20.4                | 0.0487               |
| Au-45nm | 63.3                | 11.8                | 0.0330               |

**B**

| Measured UV absorption |           |           |           |
|------------------------|-----------|-----------|-----------|
|                        | 10 × 39   | 10 × 41   | 10 × 45   |
| Transverse peak (nm)   | 512       | 510       | 509       |
| Longitudinal peak (nm) | 783       | 805       | 831       |
| Product specification  |           |           |           |
|                        | 10 × 39   | 10 × 41   | 10 × 45   |
| Transverse abs. (nm)   | 507 ~ 517 | 507 ~ 517 | 505 ~ 520 |
| Longitudinal abs. (nm) | 765 ~ 794 | 794 ~ 829 | 825 ~ 875 |
| Peak (nm)              | 780       | 808       | 850       |